https://doi.org/10.5194/egusphere-2022-761
Preprint. Discussion started: 22 August 2022

Monitoring snowpack SWE and temperature using RFID tags as wireless sensors

Mathieu Le Breton[1,2], Éric Larose[1], Laurent Baillet[1], Yves Lejeune[3], Alec van Herwijnen[4]
[1]ISTerre, Univ. Grenoble Alpes, CNRS, Grenoble, F-38000, France
[2]Géolithe Innov, Géolithe, Crolles, F-38920, France
[3]CEN-CNRM, Météo-France, CNRS, Saint-Martin-d'Hères, F-38400, France
[4]WSL Institute for Snow and Avalanche Research SLF, Davos, 7260, Switzerlanld

Correspondence to: Mathieu Le Breton (mathieu.lebreton@geolithe.com)

Abstract. This work shows that passive radio-frequency identification (RFID) tags can be used as low-cost contactless sensors, to measure the variations in snow water equivalent (SWE) of a snowpack. RFID tags are produced massively to remotely identify industrial goods, hence are available commercially off-the-shelf at very low-cost. The introduced measurement system consists of a vertical profile of RFID tags installed before the first snowfall, interrogated continuously by a 865–868 MHz reader that remains above the snowpack. The system deduces the SWE variations from the increase of phase delay induced by the new layers of fresh snow which slows the propagation of the waves. The method is tested both in a controlled laboratory environment, and outdoors on the French national reference center of Col de Porte, to cross-check the results against a solid reference dataset (cosmic rays, precipitation weighting, temperature monitoring, and snow pit surveys). The technical challenges solved concern multipathing interferences, snowmelt acceleration during reheats, measurement discontinuity, and wet snow influence. This non-contact and non-destructive RFID technique can estimate the SWE of dry snow, with the accuracy of ±3−30 kg/m2 depending on the number of tags and antennas. In addition, the system can monitor the snow temperature with 1 °C accuracy and spatialization, using dedicated sensors embedded in the tags.

1 Introduction

Measuring the snow water equivalent (SWE) of the snowpack is important for a variety of applications. At the scale of the hydrological basin, water resources and hydropower management use the SWE to estimate the reservoir of liquid water contained in the snow. At a smaller scale, avalanche risk monitoring or structural health monitoring of large buildings can also benefit from SWE monitoring. Snow and meteorological research also needs to monitor the snowpack to understand its physical processes. The SWE is one of the main macro properties of snow (Fierz et al., 2009). It is expressed as a surface density $SWE=z\rho$ (in kg/m2) and depends on the snow density ρ and to the snow depth z .

Several methods exist to estimate the SWE (Kinar and Pomeroy, 2015; Pirazzini et al., 2018). A common in-situ measurement technique is the snow course which entails taking multiple samples of the snowpack at multiple locations. However, this method is destructive, requires a lot of human resources and does not provide continuous measurements. Alternatively,

https://doi.org/10.5194/egusphere-2022-761
Preprint. Discussion started: 22 August 2022

automatic SWE monitoring is achievable through the use of snow pillows. A large variety of non-destructive methods allow for more time-efficient measurements, such as satellite data (Tedesco, 2015), ultrasonic probes for snow depth (e.g., Ryan et al., 2008), total snow weight on the ground, or cosmic ray neutron sensing (Gugerli et al., 2019) (Table 1). Among them, radiofrequency methods allow measurements at depth, exploiting the influence of the macro snow properties of its dielectric constant. Radiofrequency technologies include local probing through the resonant frequency of antennas (Kinar and Pomeroy, 2015; Techel and Pielmeier, 2011). However, probing makes measurement of a few cm3 of snow only, it is partially destructive, and it not adapted for continuous measurement. Other radiofrequency instruments allow to characterize the snow around them, such as the GPS interferometry (Larson et al., 2009), the scatterometry (Adodo et al., 2018; Picard et al., 2018), and ground-penetrating radar (GPR) (Bradford et al., 2009). GPR measures the wave propagation delay in a volume of the snowpack, to retrieve the SWE, and recently the liquid water content, the snow depth and the average density. However, GPR requires expensive surveying instruments and expert processing, and can become difficult to interpret on irregular terrains. Buried GPS or upward GPR were also introduced for monitoring the entire snowpack based on changes in phase delay (Schmid et al., 2015). Nevertheless, these instruments remain expensive, and their powering and potential maintenance under snow can become complex. Furthermore, buried GPS or upward GPRs can monitor the SWE on one location, but are hardly scalable for spatially dense monitoring. A comparison of new-generation sensors for SWE monitoring (cosmic rays, multi-frequency radar, gamma ray monitoring, buried GNSS) showed that no method is perfect (Royer et al., 2021), therefore improvements in SWE monitoring methods are still needed.

We propose to sense SWE and snow temperature using RFID tags. Tags were initially used to identify goods remotely (Ngai et al., 2008; Tzeng et al., 2008). The RFID industry produces tags in very large quantities—18 billion tags and over 30% growth in 2021 (Halliday, 2022)— allowing for low-cost tags (typ. 0.01–20 €) and reading devices (typ. 2 k€). Therefore, tags can be used in dense arrays of wireless sensors or dispatched over large areas. A tag is basically an antenna and an ultra-low-power microchip, powered wirelessly by a reading device. When interrogated, the tag communicates its identification number to the reader using either backscattering or coupling physical principles (868 MHz backscattering in this study). Recently, tags were augmented with the capabilty to sense their environment (reviewed by Costa et al., 2021), using either a sensor connected to the tag (Hamrita and Hoffacker, 2005), the tag antenna as a sensor (Bhattacharyya et al., 2009), or the properties of the wave propagation for localization or contactless sensing (Nikitin et al., 2010; Liu et al., 2012). In earth science, RFID tags have been increasingly used to monitor various surface processes (reviewed by Le Breton et al. 2021b), such as coarse sediment transportation in rivers (Nichols, 2004; Lamarre et al., 2005), temperature fluctuations of the soil (Luvisi et al., 2016; Deng et al., 2020), soil moisture (Pichorim et al., 2018; Wang et al., 2020), landslide displacement (Le Breton et al., 2019; Charléty et al., 2022a, 2022b) and rock displacement (Le Breton et al., 2021a). The few RFID studies related to snow or frost show that tags are readable below snow under certain conditions (Le Breton, 2019) and should not suffer from long-term deterioration due to cyclic freezing/thawing (Gutierrez et al., 2013). The communication quality is however altered by transmission through snow, reflection at the snow-air interface, and multipathing interferences (Le Breton, 2019) and by the presence of snow/frost

https://doi.org/10.5194/egusphere-2022-761
Preprint. Discussion started: 22 August 2022

on the tags (Nummela et al., 2008). Wagih and Shi (2021) exploited this last influence to sense—in the laboratory—the quantity of frost deposit on the tags antenna. However antenna-based sensing can characterize only the material touching the tag or a few millimeters away, and not the total volume of a snowpack. On the opposite, contactless sensing might provide information in the volume, by monitoring the changes in the signal propagation between the tag and the reader (see the review of Le Breton et al., 2021b). To date, contactless sensing was used to detect the presence and position of a human body through qualitative changes in the signal (e.g., Ruan et al., 2015; Chen et al., 2020).

We use contactless sensing instead to quantify the changes along time of a medium's physical properties—the snow water equivalent (SWE). The method introduced monitors the phase delay of a wave propagating between an RFID reader and several tags. Indeed, a Radiofrequency signal transmitting across snow slows down as the snow density increase (e.g., Le Breton et al., 2019). The SWE variations can therefore be estimated from the phase delay variation, on a snowpack that is dry or almost dry, as with buried GPR or GNSS. Besides, we also use tags as small temperature sensors (like, for example, Bagshaw et al., 2018), to monitor the vertical temperature repartition of the snowpack. This study not only introduces a new concept of RFID contactless sensing, but it is the first study that validates it in a real environment on the long term.

This article shows that given their previous placement before the snow fall, RFID tags provide a simple way to measure temperature and SWE variations locally. The tags that are wireless, have low thermal signature, and use either long-lasting or no batteries. Compared to SWE monitoring techniques such as GPR, GPS or cosmic ray sensing, RFID has the potential to provide spatialized data of SWE and temperature. Section 0 first describes the theory and instruments. Section 0 validate the principles and presents the processing steps applied, with preliminary observations in the laboratory and on the Col de Porte reference field. Finally, section 0 shows the final results of SWE and temperature measurements using the RFID system, and validate it against reference measurements over the entire 2019–2020 snow season at Col de Porte.

2 Method and instruments

2.1 Theory: from phase delay to SWE

This section presents the basic theory of microwave propagation in a dielectric medium (Balanis, 2012), applicable for snow in the 800-1000 MHz range. Electromagnetic wave propagation in snow depends mostly on its dielectric permittivity

$$\varepsilon = (\varepsilon' + j\varepsilon'')\varepsilon_0 \quad (1)$$

with ε_0 the constant dielectric permittivity of vacuum (=8.854×10^{-12} Farad / m) and ε',ε'' the relative in-phase and quadrature permittivity of the snow propagating medium, respectively. The in-phase and quadrature permittivity influence respectively the wave velocity and attenuation. We name "permittivity" the relative in-phase dielectric permittivity. At the second order, the permittivity ε'_s of dry snow at 10–1000 MHz depends on its density ρ (in kg/m^3) using:

https://doi.org/10.5194/egusphere-2022-761
Preprint. Discussion started: 22 August 2022

$$\varepsilon'_s = 1 + a\rho_x + b\rho^2 \quad (2)$$

with empirical constants approximately a=1.7x10^{-3} m^3·kg^{-1}, and b=0.7 x10^{-6} m^6·kg^{-2} (Tiuri et al., 1984).

We approximate the propagation as rays, and snow as linear, isotropic and homogeneous. That is partly valid up to about 2 GHz, for which we assume a negligible influence of scattering (Bradford et al., 2009). Snow can be considered as nonmagnetic (μ=μ_0) with a negligible conductivity ($\sigma' \approx 0, \sigma'' \approx 0$) within 10^{-12}–10^{-6} S/m for dry snow (Mellor, 1977), and we approximate it as a low-loss dielectric medium ($\sigma_{eff} \ll \varepsilon_{eff}\omega$) The wave velocity v can then be expressed as function of the snow permittivity ε' and the velocity in a vacuum c (≈ 2.998·10^8 m/s) (Bradford et al., 2009)

$$v = \frac{c}{\sqrt{\varepsilon'}} \quad (3)$$

Roughly speaking, a snow density within 100−600 kg/m^3 would have a permittivity within 1.1–2.3 (i.e., a relative velocity of 0.65–0.95). Additionally, the phase ϕ (in radians) of a wave of frequency f (in Hz), propagating two ways through a medium over a distance z (in meters) equals:

$$\phi = -\frac{4\pi f}{v} z \quad (4)$$

Therefore, when a homogeneous layer of dry snow of permittivity ε' replaces a layer of air, the phase varies as:

$$\delta\phi = \phi_{snow} - \phi_{air} = -\frac{4\pi f}{c}(1 - \sqrt{\varepsilon'})z \quad (5)$$

Using the approximation of snow permittivity (2) in a homogeneous medium leads to:

$$\delta\phi = -\frac{4\pi f}{c_{air}}\left(1 - \sqrt{1 + a\rho_x + b\rho^2}\right) z \quad (6)$$

Considering a range of relatively low density of snow (50–500 kg/m^3) and the smaller importance of the quadratic term in (2), we approximate this equation with a first order Taylor expansion:

$$\delta\phi = -\frac{2\pi f}{c} a\rho z \quad (7)$$

To validate the approximation, we compute the relative error of the Taylor approximation computed using (8). The error remains below 0.5% for density of 0 to 500 kg/m^3 , which is negligible compared to the uncertainty in the density measurement and on the phase.

https://doi.org/10.5194/egusphere-2022-761
Preprint. Discussion started: 22 August 2022

$$\frac{\delta\phi - \delta\phi_{approx}}{\delta\phi} = 1 - \frac{a\rho}{2\sqrt{1 + a\rho + b\rho^2} - 1} \quad (8)$$

Knowing that $SWE = z\rho$, the variation of snow-water equivalent ΔSWE due to the multiple layers of snow that add-up during a snowfall relates to the cumulative phase variation ΔΦ, which is measured by the RFID system:

$$\Delta SWE = -\frac{c}{2\pi f a}\Delta\phi \quad (9)$$

For indication, a phase variation of −2 π corresponds to a SWE variation of +102 kg/m^2, at 865.7 MHz frequency. In addition, the system used in this study measures the phase wrapped between [0, π], with an offset ϕ_0, so that $\phi_{meas}(t) = \phi(t) + \phi_0(t) - k\pi$ with k an unknown integer, requiring some precautions. First, we assume the phase offset ϕ_0 to be stable during the time of observation, after using precautions described in (Le Breton et al., 2017). Then, the unwrapping of the phase requires continuous measurements to avoid any ambiguity which could occur if the phase varied by more than ±π/2 between two consecutive measurements.

To estimate the SWE using (9), we make the hypothesis that the variation of phase is only due to the slowness of an additional snow layer, which requires to reduce three influence factors. First, we reduce the influence of snow on the tag antenna—which can alter the phase if its properties change a few centimeters close to the tag (Dobkin and Weigand, 2005)— by observing only the tags close to the ground (3−18 cm high). This has also the advantage to reduce the influence of snow settlement. Second, we select only the periods when the snowpack is dry or almost dry. When tags are in the snowpack, it corresponds to either a snow temperature T <0 °C or a stable phase delay. Third, we quantify then reduce the influence of multipathing interferences that occurs from reflections at layer boundaries, by combining data from multiple tags and antennas at different locations. Other effects of the propagation, such as scattering in the snowpack or on snowflakes, were negligible.

2.2 Instrumentation

Two experiments are presented, in a laboratory and outdoors. Both experiments measured the increase in phase delay caused by a new layer of dry snow formed between a reader antenna (above snow) and a tag (below snow). The reader (SR420 from Impinj) emitted and received a radiofrequency signal at 865.7 MHz, through a slot antenna in the laboratory (Impinj Threshold, 8 dBi), and through two patch antennas outdoors (Kathrein, 12 dBi). The tags (Survivor B from Confidex) are passive in essence, but the models we used are assisted by a tiny battery (with several years lifetime) which increases the tag sensitivity and read range. Each tag includes an antenna which converts the RF wave into a current, to wake up and power the microcircuit embedded in the tag. The microcircuit has ultra-low power requirements (<10 µW when interrogated), and embeds a temperature sensor. During both experiments, the reader interrogates each tag during 30 ms, sequentially, following a standard RFID protocol (EPC-Gen2, Dense Miller 8). When requested by the reader, a tag communicates its unique identifier and its temperature, by backscattering and modulating the signal amplitude. For each tag, the reader also measures the phase difference

https://doi.org/10.5194/egusphere-2022-761
Preprint. Discussion started: 22 August 2022

of arrival (more simply the «phase», measured between 0-π rad) from the incoming radiofrequency signal. The retrieved data is averaged every minute for each combination of tag, antenna and frequency available. The variation of phase is later converted in a variation of SWE and cumulate over time (see section 4 and eq. (9)). Besides, each tag also measures its temperature with an internal sensor, allowing to monitor the snow temperature on multiple locations. The temperature accuracy is provided as ± 1 °C by the constructor (after calibration) and has 0.5 °C numerical resolution.

In the laboratory experiment, we placed one reader antenna and one tag on the two sides of a 40x40cm polystyrene box, respectively 1 m above and 5 cm below the box (Fig. 1). New layers of dry snow were progressively added in the box to form a snow block with an increasing thickness, until reaching approximately 25 cm. We operated the whole experiment in a dry and cold chamber (-5 °C). The snow had been previously collected outdoors, kept dry in the chamber, and sieved to add each new layer. After adding each layer, we equalized the snow surface to be planar, then we measured the total thickness and the total weight of the snow block, allowing to estimate its density. The experiment was repeated with three snow densities (230, 275, 330 kg/m^3).

To confirm the method in the field, we installed a continuous monitoring during the 2019–2020 winter, at Col de Porte, France (alt. 1325 m). In the experiment, we planted two vertical arrays of tags on the ground. Each array comprised 12 and 11 tags with 15 cm vertical spacing between each tag, starting at 3 cm and 8 cm above ground, respectively (see Fig. 2, b-c). The tags were interrogated continuously from two antennas placed above the tags at 3 m height, from 2019-10-22 to 2020-03-27. We first focused on four snowfall events during which the top layers of snow remained entirely dry, then computed the SWE over the whole winter.

Col de Porte is the French reference site for snow measurements and instrument testing (Lejeune et al., 2019), operated by the center for snow study (CEN) of Météo France. The numerous instruments and manual surveys on this site provided an exhaustive dataset on the snowpack and its environment during the experiment (see Fig. 3). The precipitation was measured by automatic weighting, and used to estimate the variation of SWE caused by a new snow layer during a snowfall. The snow height was measured with different methods: an automatic laser instrument, manual surveys in the snow pits, and manual visualization on a pole near the RFID tags. The SWE was estimated automatically every day with the cosmic ray method. The air temperature was measured with a meteorologic station, and the snow surface temperature with infrared sensors. A webcam pictured the measurement sites every hour, which we used to validate local snow melting.

https://doi.org/10.5194/egusphere-2022-761
Preprint. Discussion started: 22 August 2022

3 Preliminary observations and processing

3.1 Snow layers simulated in laboratory

The method is first validated in a laboratory experiment, where we added cumulative new layers of snow between a tag and a reader antenna. Each new layer of snow increased the SWE estimated from the RFID phase delay (Fig. 4), with a slope that depends on snow density. The densities of 230, 270 and 335 kg/m^3 correspond to dielectric permittivity's of 1.43, 1.51 and 1.64, respectively (Tiuri et al., 1984). The cumulated variation of SWE estimated from the RFID phase (Fig. 4, solid lines) appears in line with the SWE estimated from snow weighting measurement over the complete cumulated layers (Fig. 4, dashed lines).

The SWE estimated from the phase, however, oscillates around the expected linear trend, reducing the accuracy of the method on thin snow layers. The estimated variation of SWE remained within ±10 kg/m^2 of the value obtained by snow weighting (Fig. 4, dashed and solid line, respectively). This deviation oscillates with a spatial period of about half a wavelength (135−145 mm in snow for the densities considered) which corresponds to expected fringes of interferences from the wave reflected on the air-snow interface (Le Breton, 2019).

As a conclusion, uncorrected RFID phase delay should measure large SWE variations over 50 kg/m^2, corresponding to phase shift > π. At these values, the relative error should be <20% and decrease with the SWE increase. However, estimating small changes in SWE (<10 kg/m^2) requires a method to mitigate the multipathing bias, which we introduce in the next section.

3.2 Snowfalls outdoors

During the outdoor experiment, we have selected four periods of snowfall occurring during the winter of 2019–2020 (11–12 Dec., 12–13 Dec., 10 Jan., 27–28 Feb.) for which we assume that both the falling snow and the snowpack are dry. The snow dryness is checked from independent snow measurements of surface temperature, and from complementary RFID indicators of tag temperature ≤ 0 °C (Fig. 10). For each period, and for each combination of tag below snow and reader antennas, we estimate the progressive increase of SWE from the variations of phase delay, using (9). The resulting estimation of SWE is compared with the cumulated precipitation's weight and the snow depth on Fig. 5.

The SWE estimated from the RFID phase on each tag/antenna couple (Fig. 5, colored points), evolves mostly in coherence with the cumulated precipitations (black squares). However, the different curves of uncorrected SWE indicator exhibit a bias up to 30 kg/m^2 compared to the cumulated precipitation. The bias is different for each event, tag and each antenna, thus we attribute it to multipathing on the ground, snow interfaces, tags and supports. For example, on 12 Dec., the 18-cm and 23-cm-high tags provide biased SWE only from the antenna 1. Furthermore, the amplitude bias of [+ 0.5, -0.9] (11 Dec. at 18 cm and 27 Feb. at 33 cm, resp.) is consistent with the multipathing bias of [+0.5, -2.5] rad shown by Le Breton (2019). We reduce this bias to 0 to −1.5 kg/m^2 by computing a median of the measurement made from the two reader antennas and the five tags below the snowpack (Fig. 5 continuous black line). The single outlier of −7.7 kg/m^2 on period 2 can be explained by a wind of

https://doi.org/10.5194/egusphere-2022-761
Preprint. Discussion started: 22 August 2022

40 km/h that may have distributed the snow differently on the RFID installation and on the precipitation sensors. Table 2 presents the synthetic SWE, errors, and density estimations observed in these periods.

3.3 Processing the SWE over the snow season

We finally compute the SWE over a complete winter (2019–2020) at the Col de Porte. It required more processing steps, in order to handle the small data gaps (given the ±π phase ambiguity), the periods of wet snow (which also increases the phase delay), the thermal influence of the tags support (which has accelerated the snow melting twice), and the settlement of the snow.

The first step, the phase unwrapping, cumulates the phase variations over time to solve its ±n×π ambiguity. To avoid ambiguity, the phase should therefore not vary by more than $\pi/2$ between two consecutive measurements (equivalent to 51 mm of SWE in dry conditions), requiring continuous measurements. The main challenge of the unwrapping is to handle the short data gaps. These are caused by simultaneous destructive interferences and high liquid water content surrounding the tag, that both reduce the RF signal amplitude (Le Breton et al., 2019, 2017; Occhiuzzi et al., 2013). We used an automatic unwrapping, and corrected a few remaining ambiguity issues using the phase from nearby tags in case of gaps on a tag. For verification, we also ensured that the unwrapped phase came back near its initial value at the end of the season. The resulting indicator of SWE variations per single tag is shown on Fig. 6, along the measurement of SWE based on cosmic rays and on manually weighting the snow pits (Lejeune et al., 2019). Besides, the figure shows the snow depth (measured with a laser, in the pits, and from a visual pole), the lowest temperature of each day (of the air, of the tags above snow, and of the snow surface), and the daily precipitations (with the estimation of solid to liquid ratio). The resulting raw unwrapped indicator of SWE variations obtained from the three tags (Fig. 6a, continuous lines in light colors) correlate visually with the reference SWE, yet more processing steps are necessary for the final result.

The second step mitigates the role of wet snow, that would modify the phase delay and would not be differentiated from an increase of SWE. Liquid water affects the phase delay both by slowing the wave transmitted through the snowpack (e.g., Bradford et al., 2009; Tiuri et al., 1984) and by coupling with the tag antenna (Caccami et al., 2015; Le Breton et al., 2017; Le Breton, 2019). We identified the dry snow period from their constant or slowly evolving phase delay—occurring typically from midnight to 7:00. In contrast, the phase delay was constantly changing with wet snow, due to its unstable snow liquid water content (wet snow either melts or refreeze). We removed these wet snow periods, for example on 24/12, on 02/02, and most days in the presence of sunlight. Sometimes, the snowpack did not dry for 24h or more, for example after important wet precipitations. In this case, we removed the entire wet period. We made an exception for the final snow melt occurring after March 3rd. In this period the snowpack was almost always wet: the phase delay did not stabilize, and the temperature of the tag below snow remained at zero. We nevertheless wanted to provide an estimator, knowing that it would be slightly overestimated. To estimate the SWE with the best possible accuracy, we selected the driest hour of each day, as the local minimum of phase delay and air temperature. It occurred typically around 7:00. To finish this step, we averaged the SWE

https://doi.org/10.5194/egusphere-2022-761
Preprint. Discussion started: 22 August 2022

estimator over windows of 6 hours, using only the selected data. As a perspective, an algorithm might be developed to select the dry snow periods automatically, using several input parameters such as phase, signal amplitude, or temperature. Alternatively wet snow might be estimated and corrected for in the future, as already done with techniques for buried GPS or GPR (Schmid et al., 2015; Koch et al., 2019) or for moisture-sensing tags (Occhiuzzi et al., 2013; Caccami and Marrocco, 2018; Pichorim et al., 2018; Wang et al., 2020; Wagih and Shi, 2021).

The third step mitigates the acceleration of snowmelt caused by the installation. It occurred twice in the winter (from 2019-12-14 to 2019-12-19 and from 2020-02-01 to 2020-02-03), after strong wet precipitations combined with an air temperature that remained > 0 °C during several days (Fig. 6), limiting the nightly refreezing. The influence was likely due to the thermal bridge and preferential melt water snow path, caused by the tag support. The resulting increase of snowmelt was observed by picture (Fig. 7), by a non-reversible offset formed both between the RFID and reference SWE (Fig. 6), and by the offset between the snow depth and the tag temperature variations (Fig. 10). To mitigate this effect, we distinguished the three periods (1) from 2019-10-23 to 2019-10-28, (2) from 2019-12-19 to 2019-12-30, and (3) from 2020-02-03 to 2020-02-06. In the periods 2 and 3, we fixed the SWE to the value of a reference manual pit survey, marked as ref in Fig. 8. This technical issue should be resolved on a future installation by placing tags close to the ground.

The fourth and last step mitigates the multipathing bias using multiple tags. Indeed, changes in the snowpack modify the multipathing interferences, altering the phase and amplitude of RFID signals (Le Breton, 2019). Using a singe tag and antenna, we have previously observed a multipathing bias up to 10–30 kg/m^2, in laboratory and outdoor events respectively. Averaging the data from 18 couples of tags and antennas reduced the bias from 30 to 3 kg/m^2 outdoors. Therefore we averaged the data from the tags under the snowpack, and chose only the tags close to the ground to avoid a bias due to the settlement of the snow below the tag. The period 1 had several episodes with no snow or little snow, therefore we used a single tag (the lowest one, 3cm height) to integrate the SWE variations of most of the snowpack. The accuracy using a single tag (30 kg/m^3 at worst, see section 3.2) still appeared good enough to estimate the SWE variations (50 to 150 kg/m^3 during the period 1). In the periods 2 and 3, we averaged the SWE on the first three tags at 3 cm, 8 cm and 18 cm height to improve the accuracy.

To summarize, we observed and mitigated four main challenges. Combining data from multiple tags and antennas both helped to solve the phase ambiguity during short data gaps, and reduced the multipathing bias. Two recalibrations have corrected the offset due to snowmelt near the tag support during reheats (this issue should vanish in future installations). Selecting the time windows with the driest snowpack reduced the influence of wet snow. These processing steps lead to the final SWE estimator, shown in the next section.

https://doi.org/10.5194/egusphere-2022-761
Preprint. Discussion started: 22 August 2022

8 SWE and temperature results

The final SWE estimated by RFID (Fig. 8, in red) appears consistent with the cosmic ray and snow pit measurements (in gray and black). Additionally, the RFID estimator seems to provide more realistic results than the cosmic ray method during snowmelt periods: the cosmic ray estimates both soil and snow water in shallow snowpacks leading to an overestimation during snowmelt (Sigouin and Si, 2016) as seen around November 27th after mid-March. Given the accuracy of the reference method (which have their own limitations) and the spatial heterogeneity in the snowpack, we consider the results close enough to validate the RFID method. The accuracy estimated within 3−30 kg/m^2 in the preliminary result—depending on the number of tag-antenna couples—appears visually consistent with the final data obtained..

To confirm the range of snow density measurable with this method, Fig. 9 synthetize the result of different experiments with dry snow: laboratory simulations, controlled experiments on old snow (Le Breton, 2019) and fresh snowfalls. The method works for a density ranging from 70 kg/m^3 to 400 kg/m^3, with an error below ±10%, and is very likely to work also for higher densities. This error is reasonable, compared with the 5% numeric precision of the empiric formula we used to relate permittivity with snow density (Tiuri et al., 1984) (2), and with the ±9% spreading between the different empiric formulas of the literature (Di Paolo et al., 2018). In conclusion, the RFID method can measure the variations of SWE of a dry snowpack, and we tested it for 70–400 kg/m^3 density. The largest error is ±30 kg/m^3 with a single tag and antenna location, and 3 kg/m^2 using multiple positions.

As a side result, temperature measurements are shown on Fig. 10 for each tag up to 0.78 m, along with the average temperature of the tags > 0.8 m (always above snow), the air temperature, and the snow surface temperature. The temperature of tags above snow correlates well with the air temperature. Tag temperature is higher than air temperature in the sunlight and lower in the night due to radiative heat transfer, to temporary snow/ice accumulation on the tags, and to heat conduction through the tag support. When tags are in the snowpack, their temperature remains ≤ 0 °C and does not correlate with air temperature, as expected. The reccurent stabilization of the temperature at 0 °C occurring on several tags (for example on March 10th up to 38 cm) indicates that the snowpack is partially wet near the tag. During these periods, we compared the temperature measured and confirmed, around 0 °C, the ±1 °C accuracy given by the manufacturer. Tags close to the ground remained around 0 °C most of the time, indicating that the snow near the ground stays wet: again, this behavior is expected due to the heat transfer coming from the ground. However, the snow wetness near the ground should remain small most of the time because the heat flux coming from the ground is small compared to the heat needed to melt the water. After March 23rd, once the snowpack has melt entirely near the tags, the temperature of the lowest tags increases above 0 °C, as expected. These results confirm that RFID tags can monitor and spatialize the temperature, with 1 °C accuracy, opening another perspective for RFID tags to monitor the snowpack (e.g., Bagshaw et al., 2018).

https://doi.org/10.5194/egusphere-2022-761
Preprint. Discussion started: 22 August 2022

8 Conclusions

We introduced a method based on commercial off-the-shelf RFID devices that can estimate the variation of the SWE from phase measurements, under dry snow conditions, spatial variability of tags and reader antennas, and continuous measurements. In a preliminary study, we validated the method in the laboratory and with four selected outdoor snowfalls with 1 minute time resolution. We then proposed a processing workflow for long-term observations, that mitigates short data gaps, wet snow, multipath interference and offsets due to thermal influence. We validated the method by estimating the SWE of dry snow over an entire winter, with ±3–30 kg/m^2 accuracy (accuracy improves with more tags and antennas) and 6h time resolution (time resolution is larger because of the periods of wet snow removd each day). We also introduced RFID tags as a way to measure the snowpack temperature, with the accuracy of ±1 °C (manufacturer value, confirmed here at 0 °C).

The corrected results were very coherent with reference measurements of SWE (snow pits and cosmic ray) and with the temperature of air or snow surface, during the entire season. During prolonged snow melting periods, the RFID seemed to estimate the SWE variations more accurately than the reference cosmic ray method installed on the site.

From the perspective of snow research, we introduced a method to monitor the snowpack SWE and temperature. It has the advantage to use low-cost commercial off-the-shelf devices, deployable rapidly without needing to design or manufacture RFID devices. From the perspective of RFID research, we demonstrated the ability to characterize a material over its volume using contactless sensing with an array of tags. The method exploits jointly two approaches of RFID sensing: dedicated sensors for temperature and contactless sensing for SWE, to better interpret the monitored process. We also demonstrated one step further the ability of using RFID as an effective platform for outdoor sensing applications, in very harsh natural conditions. In the future, the method could be enhanced to monitor the snow liquid water content, to spatialize the measurements over large areas with a mobile reader, or to monitor other materials such as concrete or soil

Acknowledgements

We acknowledge funding from the French National Agency for research (ANR) through the LABCOM Geo3iLab project (ANR- 17- LCV2-0007-01), and the support from the company Géolithe Innov to run the experiments. We thank G. Scheiblin from ISTerre, and J. Roulle and the technical staff from Centre d'Étude de la Neige, for the support on the experiments. We thank M. Dumont, F. Karbou, D. Jongmans, E. Rey and F. Guyoton, for their interest and fruitful discussions in the early steps of the project and all along.

References

Adodo, F.I., Remy, F., Picard, G., 2018. Seasonal variations of the backscattering coefficient measured by radar altimeters over the Antarctic Ice Sheet. The Cryosphere 12, 1767–1778. https://doi.org/10.5194/tc-12-1767-2018

https://doi.org/10.5194/egusphere-2022-761
Preprint. Discussion started: 22 August 2022

Bagshaw, E.A., Karlsson, N.B., Lok, L.B., Lishman, B., Clare, L., Nicholls, K.W., Burrow, S., Wadham, J.L., Eisen, O., Corr, H., Brennan, P., Dahl-Jensen, D., 2018. Prototype wireless sensors for monitoring subsurface processes in snow and firn. Journal of Glaciology 64, 887–896. https://doi.org/10.1017/jog.2018.76

Balanis, C.A., 2012. Advanced Engineering Electromagnetics, Second Edition. ed. John Wiley and Sons.

Beaumont, R.T., 1965. Mt. Hood Pressure Pillow Snow Gage. Journal of Applied Meteorology and Climatology 4, 626–631. https://doi.org/10.1175/1520-0450(1965)004<0626:MHPPSG>2.0.CO;2

Bhattacharyya, R., Floerkemeier, C., Sarma, S., 2009. Towards tag antenna based sensing - An RFID displacement sensor, in: 2009 IEEE International Conference on RFID. pp. 95–102. https://doi.org/10.1109/RFID.2009.4911195

Bradford, J.H., Harper, J.T., Brown, J., 2009. Complex dielectric permittivity measurements from ground-penetrating radar data to estimate snow liquid water content in the pendular regime: MEASURING SWE WITH GPR. Water Resources Research 45. https://doi.org/10.1029/2008WR007341

Caccami, M.C., Manzari, S., Marrocco, G., 2015. Phase-Oriented Sensing by Means of Loaded UHF RFID Tags. IEEE Transactions on Antennas and Propagation 63, 4512–4520. https://doi.org/10.1109/TAP.2015.2465891

Caccami, M.C., Marrocco, G., 2018. Electromagnetic Modeling of Self-Tuning RFID Sensor Antennas in Linear and Nonlinear Regimes. IEEE Transactions on Antennas and Propagation 66, 2779–2787. https://doi.org/10.1109/TAP.2018.2820322

Charléty, A., Le Breton, M., Larose, E., Baillet, L., 2022a. 2D Phase-Based RFID Localization for On-Site Landslide Monitoring. Remote Sensing 14, 3577. https://doi.org/10.3390/rs14153577

Charléty, A., Mathieu, L.B., Larose, É., Baillet, L., 2022b. Long-term Monitoring of Soil Surface Deformation with RFID. Cagliary, Italy.

Chen, Z., Yang, P., Xiong, J., Feng, Y., Li, X.-Y., 2020. TagRay: Contactless Sensing and Tracking of Mobile Objects using COTS RFID Devices, in: IEEE INFOCOM 2020 - IEEE Conference on Computer Communications. pp. 307–316. https://doi.org/10.1109/INFOCOM41043.2020.9155531

Costa, F., Genovesi, S., Borgese, M., Michel, A., Dicandia, F.A., Manara, G., 2021. A Review of RFID Sensors, the New Frontier of Internet of Things. Sensors 21, 3138. https://doi.org/10.3390/s21093138

Deng, F., Zuo, P., Wen, K., Wu, X., 2020. Novel soil environment monitoring system based on RFID sensor and LoRa. Computers and Electronics in Agriculture 169, 105169. https://doi.org/10.1016/j.compag.2019.105169

Denoth, A., 1994. An electronic device for long-term snow wetness recording. Annals of Glaciology 19, 104–106. https://doi.org/10.3189/S0260305500011058

Di Paolo, F., Cosciotti, B., Lauro, S.E., Mattei, E., Pettinelli, E., 2018. Dry snow permittivity evaluation from density: A critical review, in: 2018 17th International Conference on Ground Penetrating Radar (GPR). pp. 1–5. https://doi.org/10.1109/ICGPR.2018.8441610

Dobkin, D., Weigand, S., 2005. Environmental effects on RFID tag antennas, in: IEEE MTT-S Int. Microwave Symp. Dig. Long Beach, CA, USA, pp. 135–138. https://doi.org/10.1109/MWSYM.2005.1516541

https://doi.org/10.5194/egusphere-2022-761
Preprint. Discussion started: 22 August 2022

Essery, R., Morin, S., Lejeune, Y., B Ménard, C., 2013. A comparison of 1701 snow models using observations from an alpine site. Advances in Water Resources, Snow–Atmosphere Interactions and Hydrological Consequences 55, 131–148. https://doi.org/10.1016/j.advwatres.2012.07.013

Fierz, C., Amstrong, R.L., Durand, Y., Etchevers, P., Greene, E., McClung, D.M., Nishimura, K., Satyawali, P.K., Sokratov, S.A., 2009. The International Classification for Seasonal Snow on the Ground (No. IHP-VII Technical Documents in Hydrology N°83, IACS Contribution N°1). UNESCO-IHP, Paris.

Gugerli, R., Salzmann, N., Huss, M., Desilets, D., 2019. Continuous and autonomous snow water equivalent measurements by a cosmic ray sensor on an alpine glacier. The Cryosphere 22.

Gutierrez, A., Nicolalde, F.D., Ingle, A., Hochschild, W., Veeramani, R., Hohberger, C., Davis, R., 2013. High-frequency RFID tag survivability in harsh environments, in: IEEE Int. Conf. on RFID. Penang, Malaysia, pp. 58–65. https://doi.org/10.1109/RFID.2013.6548136

Halliday, S., 2022. Of Hamburgers . . . and RAIN RFID IC Tags. RAIN RFID Alliance, Steve Halliday, President of RAIN Alliance. URL https://rainrfid.org/blog/of-hamburgers-and-rain-rfid-ic-tags/ (accessed 4.18.22).

Hamrita, T.K., Hoffacker, E.C., 2005. Development of a smart wireless soil monitoring sensor prototype using RFID technology. Applied Engineering in Agriculture 21, 139–143.

Kendra, J.R., Ulaby, F.T., Sarabandi, K., 1994. Snow probe for in situ determination of wetness and density. IEEE Transactions on Geoscience and Remote Sensing 32, 1152–1159. https://doi.org/10.1109/36.338363

Kinar, N.J., Pomeroy, J.W., 2015. Measurement of the physical properties of the snowpack. Reviews of Geophysics 53, 481–544. https://doi.org/10.1002/2015RG000481

Koch, F., Henkel, P., Appel, F., Schmid, L., Bach, H., Lamm, M., Prasch, M., Schweizer, J., Mauser, W., 2019. Retrieval of Snow Water Equivalent, Liquid Water Content, and Snow Height of Dry and Wet Snow by Combining GPS Signal Attenuation and Time Delay. Water Resources Research 55, 4465–4487. https://doi.org/10.1029/2018WR024431

Koch, F., Prasch, M., Schmid, L., Schweizer, J., Mauser, W., 2014. Measuring Snow Liquid Water Content with Low-Cost GPS Receivers. Sensors 14, 20975–20999. https://doi.org/10.3390/s141120975

Lamarre, H., MacVicar, B., Roy, A.G., 2005. Using Passive Integrated Transponder (PIT) Tags to Investigate Sediment Transport in Gravel-Bed Rivers. Journal of Sedimentary Research 75, 736–741. https://doi.org/10.2110/jsr.2005.059

Larson, K.M., Gutmann, E.D., Zavorotny, V.U., Braun, J.J., Williams, M.W., Nievinski, F.G., 2009. Can we measure snow depth with GPS receivers? Geophys. Res. Lett. 36, L17502. https://doi.org/10.1029/2009GL039430

Le Breton, M., 2019. Suivi temporel d'un glissement de terrain à l'aide d'étiquettes RFID passives, couplé à l'observation de pluviométrie et de bruit sismique ambiant (PhD Thesis). Université Grenoble Alpes, ISTerre, Grenoble, France.

Le Breton, M., Baillet, L., Larose, E., Rey, E., Benech, P., Jongmans, D., Guyoton, F., 2017. Outdoor UHF RFID: Phase Stabilization for Real-World Applications. IEEE Journal of Radio Frequency Identification 1, 279–290. https://doi.org/10.1109/JRFID.2017.2786745

https://doi.org/10.5194/egusphere-2022-761
Preprint. Discussion started: 22 August 2022

Le Breton, M., Baillet, L., Larose, E., Rey, E., Benech, P., Jongmans, D., Guyoton, F., Jaboyedoff, M., 2019. Passive radio-frequency identification ranging, a dense and weather-robust technique for landslide displacement monitoring. Engineering Geology 250, 1–10. https://doi.org/10.1016/j.enggeo.2018.12.027

Le Breton, M., Grunbaum, N., Baillet, L., Larose, É., 2021a. Monitoring rock displacement threshold with 1-bit sensing passive RFID tag (No. EGU21-15305). Copernicus Meetings. https://doi.org/10.5194/egusphere-egu21-15305

Le Breton, M., Liébault, F., Baillet, L., Charléty, A., Larose, É., Tedjini, S., 2021b. Dense and long-term monitoring of Earth surface processes with passive RFID -- a review. https://arxiv.org/abs/2112.11965

Lejeune, Y., Dumont, M., Panel, J.-M., Lafaysse, M., Lapalus, P., Le Gac, E., Lesaffre, B., Morin, S., 2019. 57 years (1960–2017) of snow and meteorological observations from a mid-altitude mountain site (Col de Porte, France, 1325 m of altitude). Earth System Science Data 11, 71–88. https://doi.org/10.5194/essd-11-71-2019

Liu, Y., Zhao, Y., Chen, L., Pei, J., Han, J., 2012. Mining Frequent Trajectory Patterns for Activity Monitoring Using Radio Frequency Tag Arrays. IEEE Transactions on Parallel and Distributed Systems 23, 2138–2149. https://doi.org/10.1109/TPDS.2011.307

Luvisi, A., Panattoni, A., Materazzi, A., 2016. RFID temperature sensors for monitoring soil solarization with biodegradable films. Computers and Electronics in Agriculture 123, 135–141. https://doi.org/10.1016/j.compag.2016.02.023

Mellor, M., 1977. Engineering Properties of Snow. Journal of Glaciology 19, 15–66. https://doi.org/10.1017/S002214300002921X

Nichols, M.H., 2004. A Radio Frequency Identification System for Monitoring Coarse Sediment Particle Displacement. Applied Engineering in Agriculture 20, 783–787. https://doi.org/10.13031/2013.17727

Nikitin, P.V., Martinez, R., Ramamurthy, S., Leland, H., Spiess, G., Rao, K.V.S., 2010. Phase based spatial identification of UHF RFID tags, in: IEEE Int. Conf. RFID. IEEE, Orlando, FL, USA, pp. 102–109. https://doi.org/10.1109/RFID.2010.5467253

Nummela, J., Ukkonen, L., Sydänheimo, L., 2008. Passive UHF RFID tags in arctic environment. International Journal of Communications 2, 135–142.

Occhiuzzi, C., Caizzone, S., Marrocco, G., 2013. Passive UHF RFID antennas for sensing applications: Principles, methods, and classifcations. IEEE Antennas and Propagation Magazine 55, 14–34. https://doi.org/10.1109/MAP.2013.6781700

Picard, G., Sandells, M., Löwe, H., 2018. SMRT: an active–passive microwave radiative transfer model for snow with multiple microstructure and scattering formulations (v1.0). Geoscientific Model Development 11, 2763–2788. https://doi.org/10.5194/gmd-11-2763-2018

Pichorim, S., Gomes, N., Batchelor, J., 2018. Two Solutions of Soil Moisture Sensing with RFID for Landslide Monitoring. Sensors 18, 452. https://doi.org/10.3390/s18020452

Pirazzini, R., Leppänen, L., Picard, G., Lopez-Moreno, J.I., Marty, C., Macelloni, G., Kontu, A., von Lerber, A., Tanis, C.M., Schneebeli, M., de Rosnay, P., Arslan, A.N., 2018. European In-Situ Snow Measurements: Practices and Purposes. Sensors (Basel) 18. https://doi.org/10.3390/s18072016

https://doi.org/10.5194/egusphere-2022-761
Preprint. Discussion started: 22 August 2022

Royer, A., Roy, A., Jutras, S., Langlois, A., 2021. Review article: Performance assessment of radiation-based field sensors for monitoring the water equivalent of snow cover (SWE). The Cryosphere 20.

Ruan, W., Yao, L., Sheng, Q.Z., Falkner, N., Li, X., Gu, T., 2015. TagFall: Towards Unobstructive Fine-Grained Fall Detection based on UHF Passive RFID Tags, in: Proceedings of the 12th EAI International Conference on Mobile and Ubiquitous Systems: Computing, Networking and Services. ACM, Coimbra, Portugal. https://doi.org/10.4108/eai.22-7-2015.2260072

Ryan, W.A., Doesken, N.J., Fassnacht, S.R., 2008. Evaluation of Ultrasonic Snow Depth Sensors for U.S. Snow Measurements. Journal of Atmospheric and Oceanic Technology 25, 667–684. https://doi.org/10.1175/2007JTECHA947.1

Schattan, P., Köhli, M., Schrön, M., Baroni, G., Oswald, S.E., 2019. Sensing Area-Average Snow Water Equivalent with Cosmic-Ray Neutrons: The Influence of Fractional Snow Cover. Water Resources Research 55, 10796–10812. https://doi.org/10.1029/2019WR025647

Schmid, L., Heilig, A., Mitterer, C., Schweizer, J., Maurer, H., Okorn, R., Eisen, O., 2014. Continuous snowpack monitoring using upward-looking ground-penetrating radar technology. Journal of Glaciology 60, 509–525. https://doi.org/10.3189/2014JoG13J084

Schmid, L., Koch, F., Heilig, A., Prasch, M., Eisen, O., Mauser, W., Schweizer, J., 2015. A novel sensor combination (upGPR-GPS) to continuously and nondestructively derive snow cover properties. Geophysical Research Letters 42, 3397–3405. https://doi.org/10.1002/2015GL063732

Sigouin, M.J.P., Si, B.C., 2016. Calibration of a non-invasive cosmic-ray probe for wide area snow water equivalent measurement. The Cryosphere 10, 1181–1190. https://doi.org/10.5194/tc-10-1181-2016

Sihvola, A., Tiuri, M., 1986. Snow Fork for Field Determination of the Density and Wetness Profiles of a Snow Pack. IEEE Transactions on Geoscience and Remote Sensing GE-24, 717–721. https://doi.org/10.1109/TGRS.1986.289619

Techel, F., Pielmeier, C., 2011. Point observations of liquid water content in wet snow – investigating methodical, spatial and temporal aspects. The Cryosphere 5, 405–418. https://doi.org/10.5194/tc-5-405-2011

Tedesco, M., 2015. Remote Sensing of the Cryosphere, 1st ed, The Cryosphere Science Series. Wiley.

Tedesco, M., Derksen, C., Deems, J.S., Foster, J.L., 2014. Remote sensing of snow depth and snow water equivalent, in: Remote Sensing of the Cryosphere. John Wiley & Sons, Ltd, pp. 73–98. https://doi.org/10.1002/9781118368909.ch5

Tiuri, M., Sihvola, A., Nyfors, E., Hallikaiken, M., 1984. The complex dielectric constant of snow at microwave frequencies. IEEE Journal of Oceanic Engineering 9, 377–382. https://doi.org/10.1109/JOE.1984.1145645

Wagih, M., Shi, J., 2021. Wireless Ice Detection and Monitoring Using Flexible UHF RFID Tags. IEEE Sensors Journal 21, 18715–18724. https://doi.org/10.1109/JSEN.2021.3087326

Wang, J., Chang, L., Aggarwal, S., Abari, O., Keshav, S., 2020. Soil moisture sensing with commodity RFID systems, in: Proceedings of the 18th International Conference on Mobile Systems, Applications, and Services. ACM, Toronto Ontario Canada, pp. 273–285. https://doi.org/10.1145/3386901.3388940

https://doi.org/10.5194/egusphere-2022-761
Preprint. Discussion started: 22 August 2022

Table 1: Methods to estimate SWE, compared with the introduced RFID method.

Method	Direct measurement	Area	Manual/auto	Comments	References
Sampling	Weight	cm ^{2}	manual	Destructive, time consuming.	(Kinar and Pomeroy, 2015)
Pillow	Weight	m^2	auto		(Beaumont, 1965; Kinar and Pomeroy, 2015)
Cosmic ray	Neutron counting	m^2	auto		(Schattan et al., 2019; Royer et al., 2021)
Gamma ray scintillator	Radioactive emissions	m^2	auto	Safety issues if a source is used.	(Royer et al., 2021)
Models	Snow depth, T°C …	m^2	auto		(Essery et al., 2013)
Probe	Permittivity (detuning)	cm ^{2}	manual		(Sihvola and Tiuri, 1986; Kendra et al., 1994; Denoth, 1994)
Radar	Permittivity (delay)	m^2	manual/auto		(Schmid et al., 2014; Royer et al., 2021)
GNSS	Permittivity (delay)	m-km^2	auto		(Koch et al., 2014, 2019; Royer et al., 2021)
Satellite	Permittivity, gravity …	km^2	auto	Various methods	(Tedesco et al., 2014)
RFID	**Permittivity (delay)**	**dm^2**	**auto**	**Low-cost passive T°C sensor**	**This study**

Table 2: Synthesis of the variations of measurements between the start and end of each observed snowfall period. The columns represent, during (1–3) the different periods considered: (4–6) the cumulated variation of snow depth and SWE, (7) RMS error of all single-tag measurement compared with precipitations, (8) Error between the SWE from multi-tag median and the precipitations. (9–10) the density of the new layer is also estimated, only for the periods 1_{half} and 3 which occurred >24 hours after the previous snowfall. In other periods, the density computation is not applicable (na) due to compaction.

Period	Start	End	Δh m	ΔSWE precip kg·m^{-2}	ΔSWE RFID kg·m^{-2}	RFID error 1x RMS Single tag	RFID Error Multi-tags	Density from precip. kg/m^3	Density from RFID kg/m^3
1_{half}	11/12 12:00	11/12 21:00	0.14	17.4	15.8	6.5	-1.5	116	128
1	11/12 12:00	12/12 10:00	0.08	5.7	5.5	2.1	-0.2	na	na
2	12/12 18:00	13/12 08:00	0.15	44.5	36.8	5.6	-7.7	na	na
3	10/01 03:00	10/01 09:30	0.07	4.6	4.6	3.6	0	65	65
4	27/02 11:00	27/02 16:00	0.06	16.1	14.6	11	-1.5	na	na

https://doi.org/10.5194/egusphere-2022-761
Preprint. Discussion started: 22 August 2022

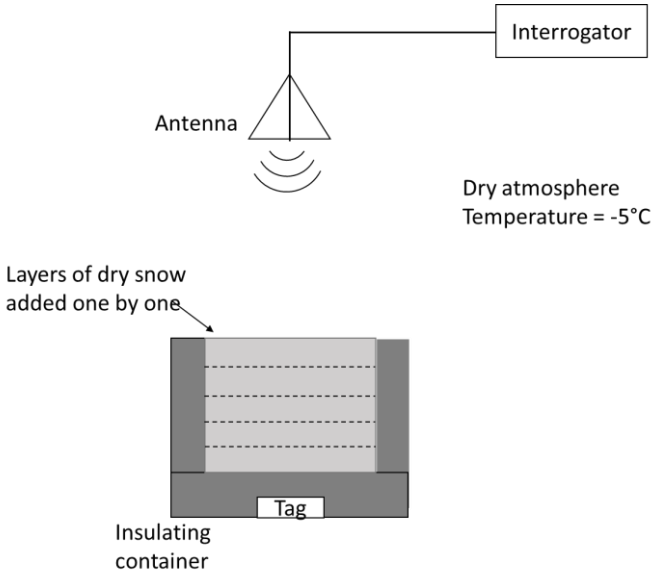

475

Fig. 1: Experimental setup to measure the effect of a new layer of snow, simulated in a laboratory. The dry snow layer between the tag and the reader antenna increases the phase delay of the Radiofrequency signal.

https://doi.org/10.5194/egusphere-2022-761
Preprint. Discussion started: 22 August 2022

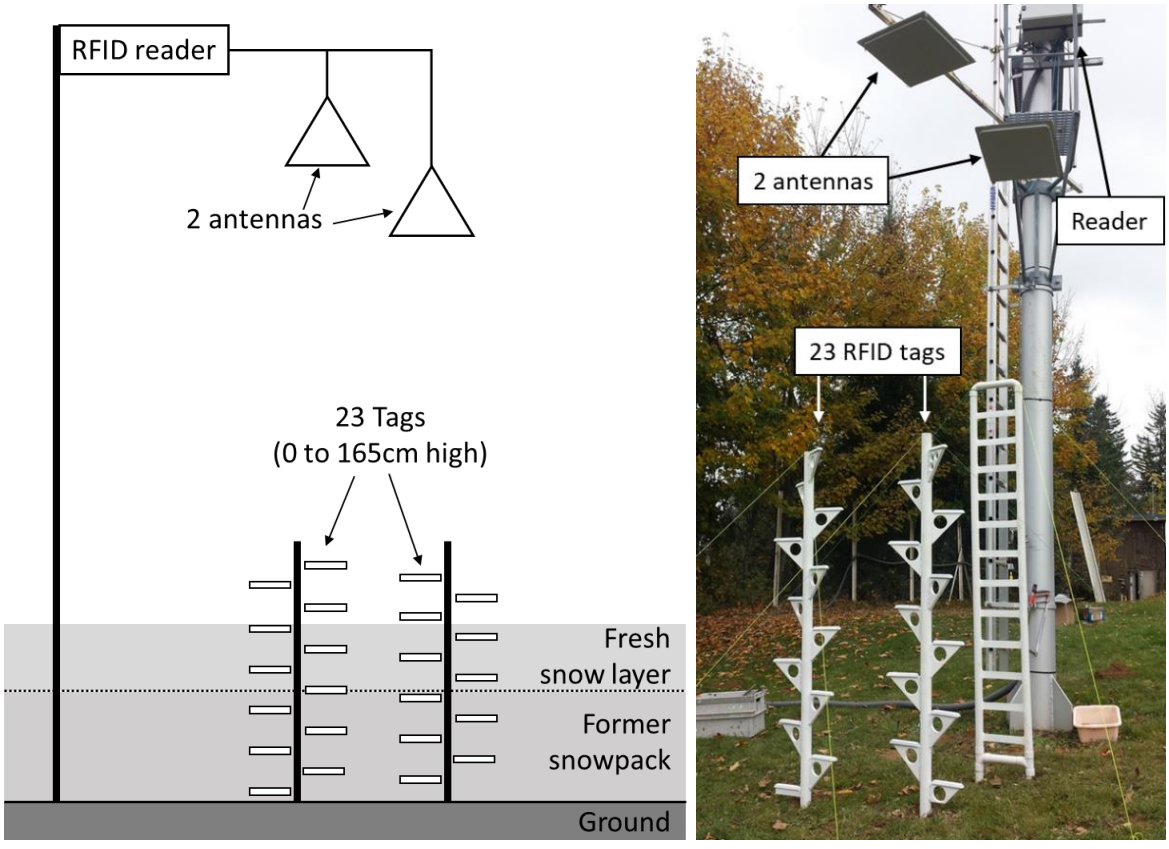

480 **Fig. 2: Experimental setup to measure the SWE variations outdoors.**

https://doi.org/10.5194/egusphere-2022-761
Preprint. Discussion started: 22 August 2022

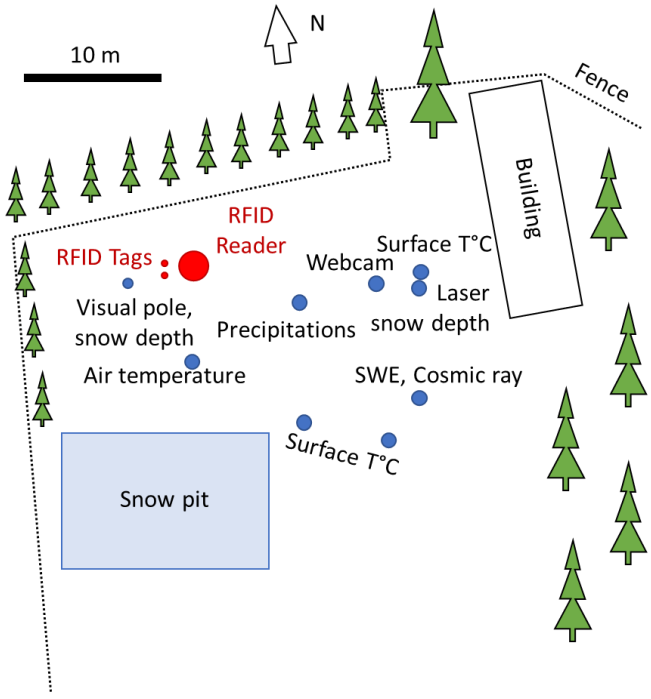

Fig. 3: Site of col de Porte, with the position of the reference instruments highlighted. Modified from Lejeune et al. (2019)

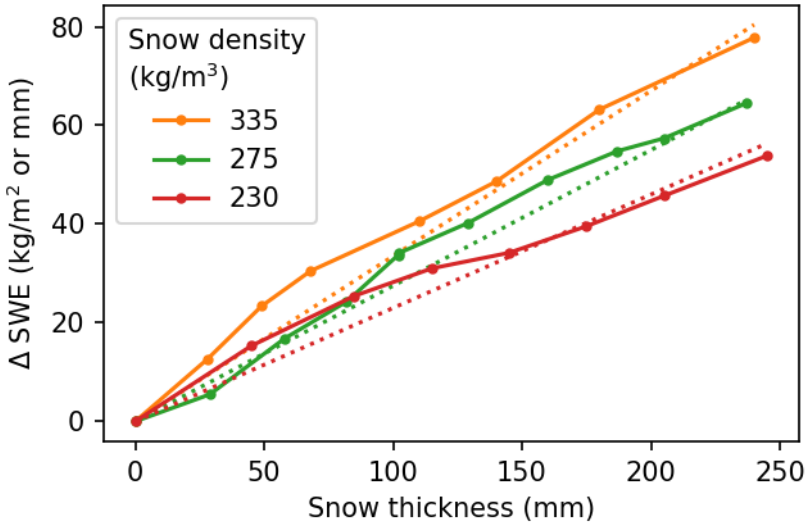

485

Fig. 4: Cumulated variations of SWE estimated from the measured snow density (dashed line) and from the RFID phase measurement (solid lines connecting round points), as function of the thickness of the snow block (9 layers for 275 kg/m³, 7 layers for 335 kg/m³, and 230 kg/m³). Three densities of dry snow are considered.

https://doi.org/10.5194/egusphere-2022-761
Preprint. Discussion started: 22 August 2022

490

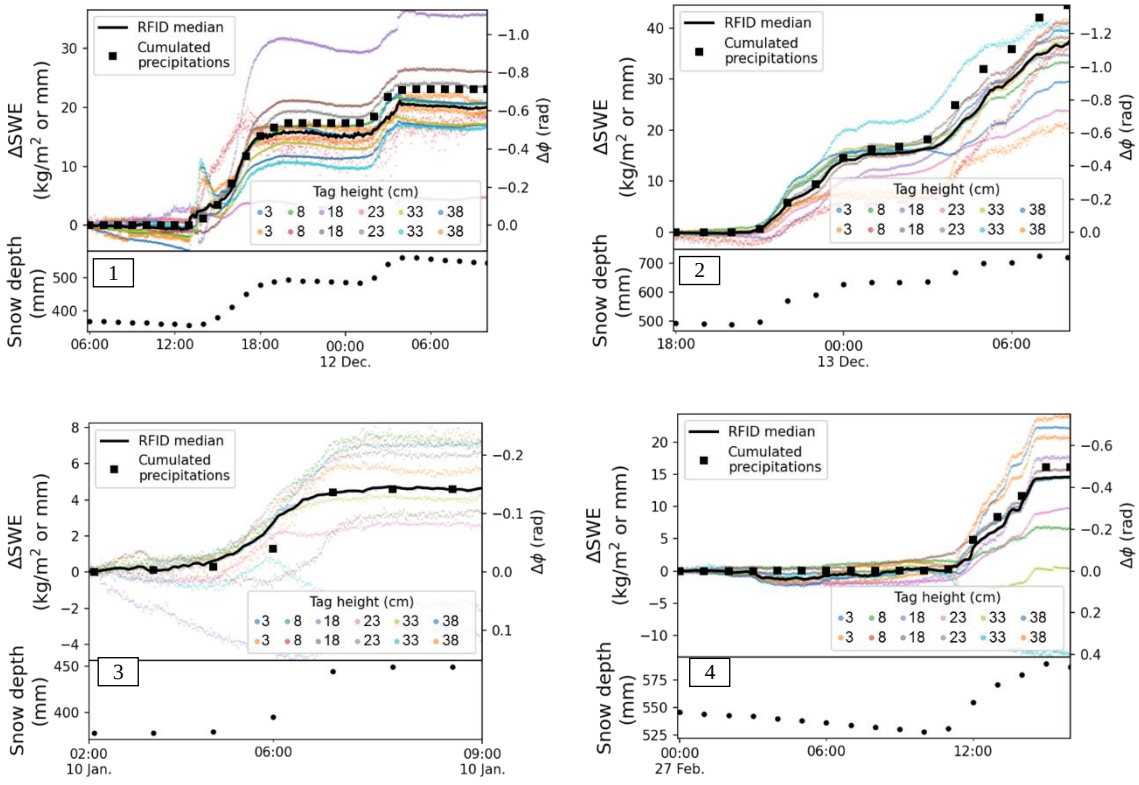

495 **Fig. 5: Cumulated variation of SWE estimated during four snowfall events of the 2019–2020 winter for which we expect purely dry fresh snow. SWE is expressed both as the surfacic mass of snow (kg/m^2) and as its equivalent water column thickness (in mm). The two phase values shown for the same tag are measured from two antennas, 1 (top color) and 2 (bottom color). The data is presented along with the SWE estimated from cumulated precipitations (obtained by automatic weighting) and the snow depth (by a laser sensor) measured on site.**

https://doi.org/10.5194/egusphere-2022-761
Preprint. Discussion started: 22 August 2022

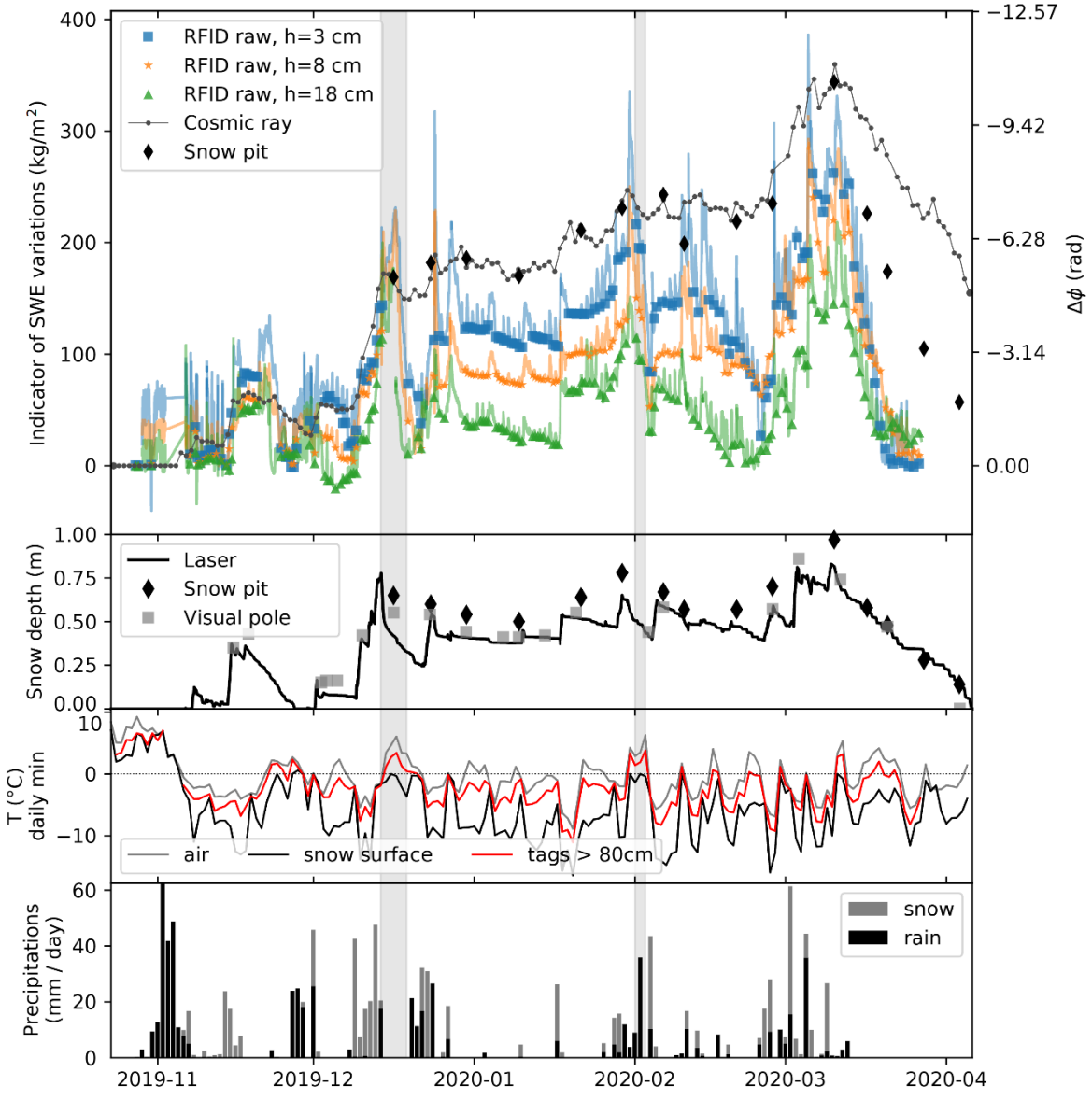

Fig. 6: Raw indicator of SWE variations, with their equivalent variation of phase delay, for the snowpack located above the tags at 3, 8 and 18 cm from the ground. We removed the periods of wet snowpack (peaks on the raw SWE indicators), and only the colored markers are accounted to estimate the SWE. SWE is also measured with automatic cosmic ray neutron counting and with snow pit surveys. The figure also shows the snow depth, daily minimum temperature, and precipitations. In the grayed periods, a reheat accelerated the snowpack melting around the tags support.

https://doi.org/10.5194/egusphere-2022-761
Preprint. Discussion started: 22 August 2022

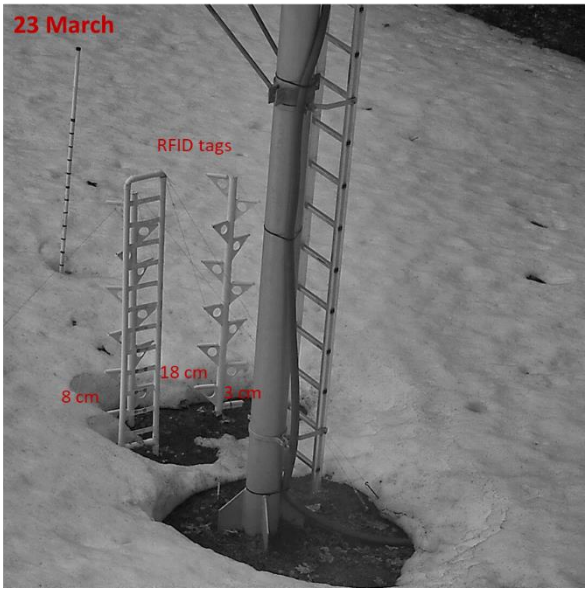

Fig. 7: Photography of the monitoring installation taken from the webcam, on 23/03 at midday, the which confirms that the snowpack has melted faster around the tag supports, and that there is no more snow around the tags on 23/03.

510

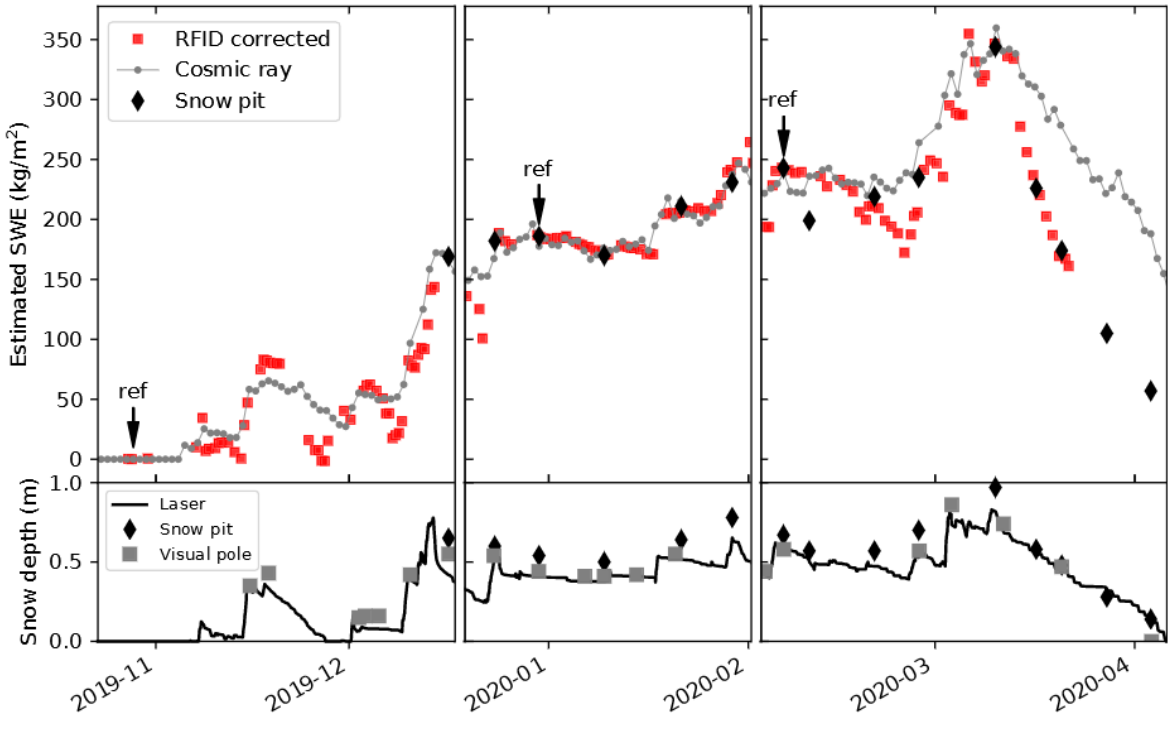

Fig. 8: Measurements for the three periods of (top) SWE with RFID keeping only driest snowpack time windows, cosmic rays and snow pit survey. (bottom) Snow depth measured at three locations using a laser sensor, manual surveying and a visual pole. In the

https://doi.org/10.5194/egusphere-2022-761
Preprint. Discussion started: 22 August 2022

first period, the data comes only from the 3 cm high tag, due to the lower snow depth. In the following periods, the data is averaged from the three lowest tags (3 cm, 8 cm and 18 cm). In each period, we calibrated the SWE RFID estimation with a reference SWE based on a manual measurement, indicated by an arrow.

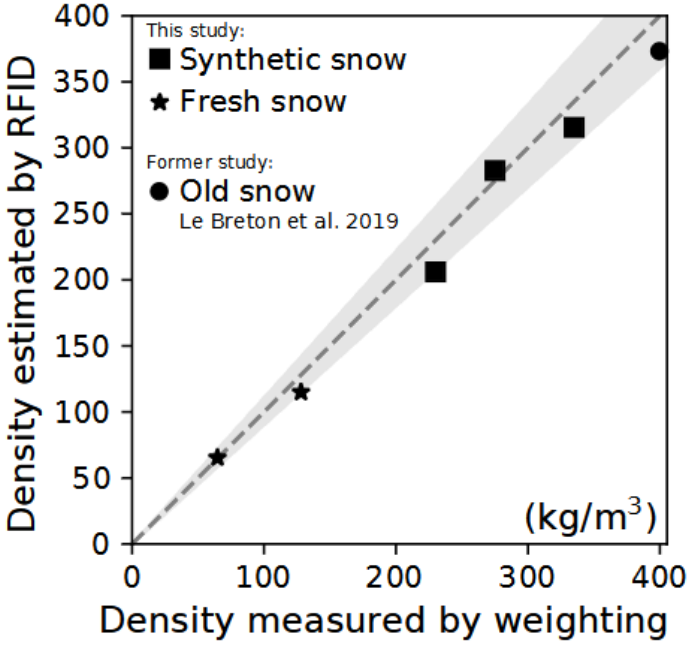

Fig. 9: Comparison of the density of the new layer in each observation (knowing its thickness), estimated either from the weight and volume of a snow sample, or from the RFID phase difference. The gray zone represents ±11% around the ideal value. This confirms the ability to measure different types of dry snow, from light fresh snow to heavier compacted snow.

https://doi.org/10.5194/egusphere-2022-761
Preprint. Discussion started: 22 August 2022

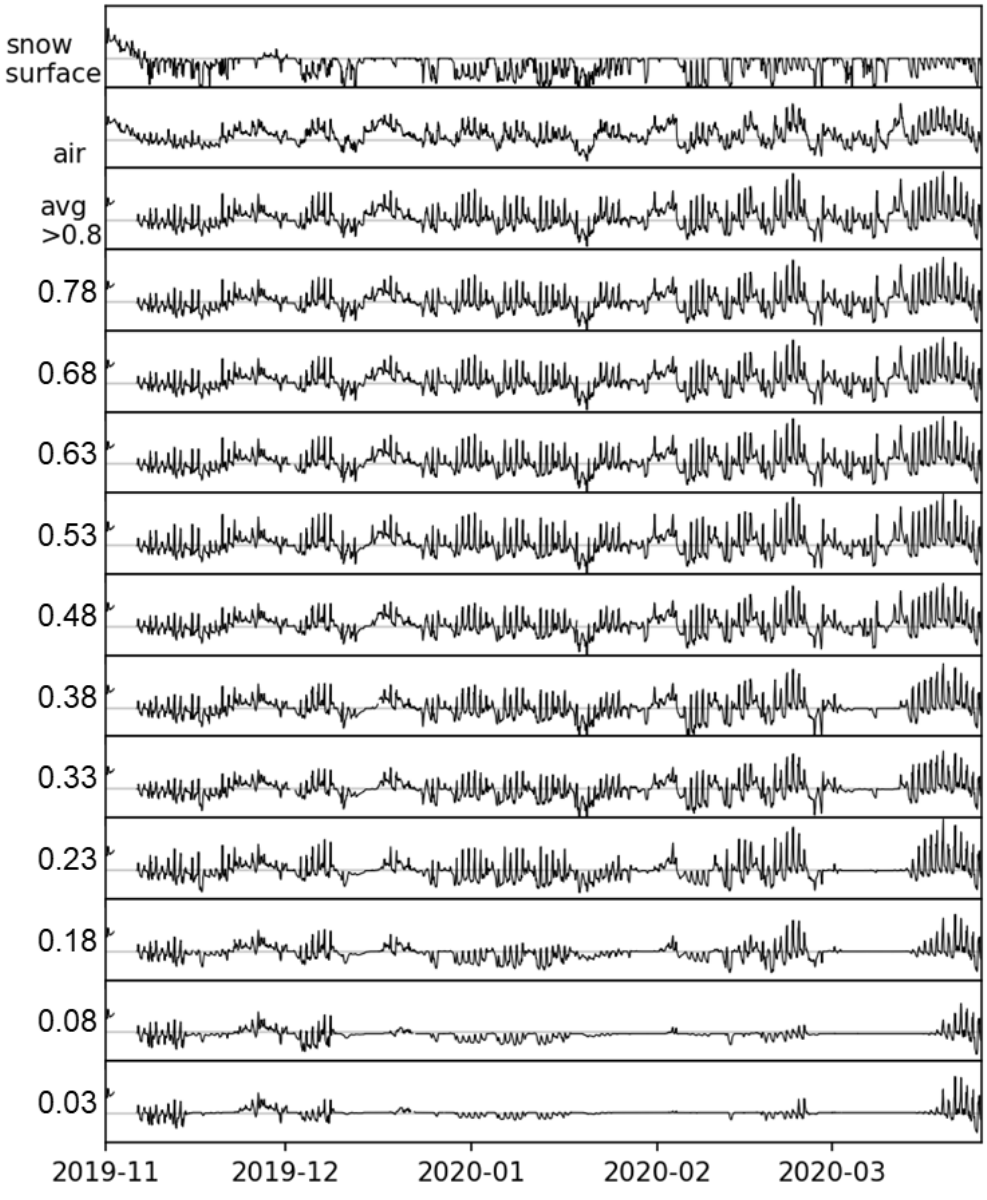

525 **Fig. 10: Measurement of temperature made on each tag, from 0 to 0.78 m above ground, as well as the average temperature of tags above 0.8 m, the air temperature measured by meteorologic station, and the temperature of the snow (or soil) surface measured by infrared. The y-axis ranges from -12 °C to +22 °C on each graph.**